

Electronic Communication between Two Amine Redox Centers Bridged by a Bis(terpyridine)ruthenium(II) Complex

Chang-Jiang Yao, Jiannian Yao, and Yu-Wu Zhong*

Beijing National Laboratory for Molecular Sciences, CAS Key Laboratory of Photochemistry, Institute of Chemistry, Chinese Academy of Sciences, Beijing 100190, People's Republic of China

S Supporting Information

ABSTRACT: Two bis(terpyridine)ruthenium(II) complexes **2** and **3** appended with one or two di-*p*-anisylamino groups, respectively, were synthesized and fully characterized. Their electronic properties were studied by electrochemical and spectroscopic analyses. Electronic communication between individual amine sites of **3** was estimated by intervalence charge-transfer band analyses.

Mixed-valence (MV) compounds have been the subject of enormous research activities in the past 4 decades.¹ In comparison with the extensively studied inorganic and organometallic binuclear complexes,² organic MV compounds have remained relatively unexplored. Among numerous organic redox groups,³ triarylamine have gained increasing attention in the studies of MV systems,⁴ in addition to their widespread applications in optoelectronic devices.⁵ On the other hand, transition-metal polyazine complexes have attracted extensive interest because of their superior photophysical and electrochemical properties.⁶ Linear coordination oligomers consisting of multiple octahedral Ru atoms have recently been studied as single-molecular wires.⁷ We report herein the electronic communication of two di-*p*-anisylamino redox centers coupled through a polyazine transition-metal motif [Ru(tpy)₂], where tpy is 2,2':6',2''-terpyridine. The effect of [Ru(tpy)₂] on electronic delocalization is assessed by analyzing the intervalence charge-transfer (IVCT) transition associated with optically induced hole transfer from one triarylamine center to the other. To the best of our knowledge, this is the first example to use transition-metal polypyridyl complexes as the bridge unit to build triarylamine MV systems. However, organic MV systems bridged by a metal porphyrin⁸ or a platinum alkynyl⁹ unit have been documented.

The following considerations were taken into account when complex **3** in Scheme 1 was designed. First, 4-methoxy substituents were chosen to ensure reversible oxidation of triarylamine. Second, the Ru atom was chosen because the anodic redox potential of [Ru(tpy)₂]²⁺ is well-separated from those of triarylamine and the ligand lability is not an issue in this complex. Third, amine atoms are directly connected to tpy ligands to ensure strong coupling between them. We note that there are several reports on the Ru(tpy)–triarylamine conjugated systems.¹⁰ However, none of these intended to study the electronic coupling between amine redox centers. Ligand **1** containing a di-*p*-anisylamino motif was obtained in 78% yield through a Pd-catalyzed C–N bond formation¹¹ between

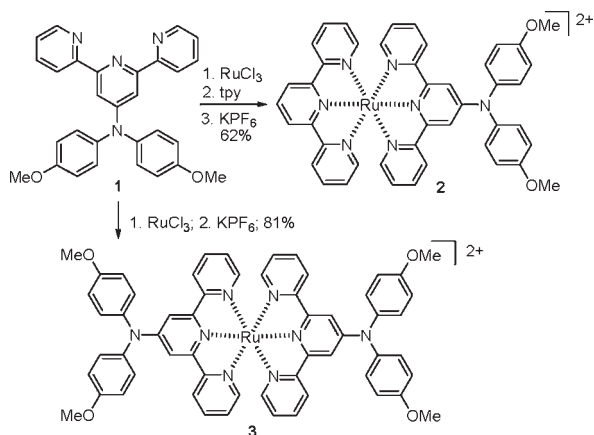
4'-bromoterpyridine and 4,4'-dimethoxydiphenylamine (see the Supporting Information for details). The reaction of RuCl₃ with 2 equiv of **1**, followed by anion exchange with KPF₆, afforded complex **3** in 81% yield. Complex **2**, with one di-*p*-anisylamino substituent, was also prepared for a comparison study. The identities of new compounds were confirmed by ¹H NMR, mass spectrometry, and microanalysis. Besides, a single crystal of complex **3** with a NO₃[−] counteranion was obtained by slowly diffusing *n*-hexane into a solution of **3** in CHCl₃, and its X-ray crystallographic structure is shown in Figure 1.¹² The N–N distance between two amino N atoms was found to be 12.26 Å.

The electronic absorption spectra of compounds **1–3** and benchmark complex [Ru(tpy)₂](PF₆)₂ are shown in Figure 2a. Ligand **1** displays an intraligand (IL) π–π* transition at 281 nm and a shoulder between 310 and 400 nm, which is assigned to the IL charge-transfer (ILCT) transition from the di-*p*-anisylamino group to the tpy moiety.¹⁰ In comparison, complexes **2** and **3** both exhibit a broad and intense band in the visible region, in addition to the slightly red-shifted and more intense IL and ILCT transitions. The broad band in the visible region is attributable to an admixture of metal-to-ligand charge-transfer (MLCT) and ligand-to-ligand charge-transfer (LLCT) transitions.¹⁰

The electronic properties of these compounds were further studied by electrochemical analysis (Table S1 and Figures S1–S4 in the Supporting Information and Figure 3). The cyclic voltammogram (CV) of ligand **1** reveals a redox couple at +0.97 V and an irreversible anodic peak at +1.41 V vs Ag/AgCl (Figure 3a). The first peak is chemically reversible, as shown by the red line, where the potential was scanned back at +1.2 V. However, a relatively large separation (110 mV) between the anodic peak and the return cathodic peak suggests a somewhat slow electron-transfer process. This peak is ascribed to the N/N^{•+} process of the di-*p*-anisylamino site. The second peak at +1.41 V is assigned to the further oxidation of the in situ generated radical cation to a dication species (N²⁺), with the production of new chemical species, which gives rise to a new peak near 0 V. Similar processes have been reported to occur from various triarylamine.^{13,14} We did not determine the identity of the decomposed product at this stage. However, some literatures prove that a carbazole derivative is produced during similar processes.¹⁴ We note that this decomposed product is also evident in the CV profile of complex **3** (Figure 3d). The anodic scan of complex **2** displays two redox couples at +0.98 and +1.44 V, respectively (Figure 3c). The former peak is attributable

Received: April 6, 2011

Published: July 07, 2011

Scheme 1. Synthesis of Compounds 1–3^a

^aThe counteranions are PF_6^- .

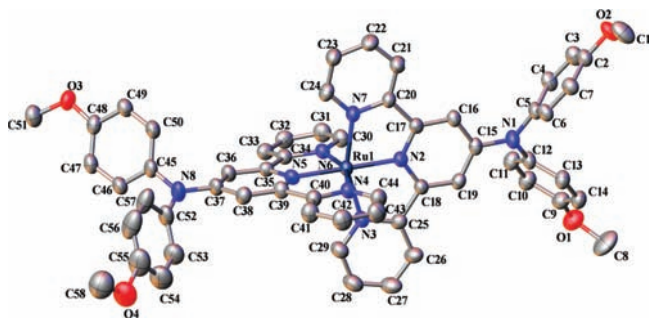


Figure 1. Thermal ellipsoid plot with 50% probability of $[\mathbf{3}](\text{NO}_3)_2$. H atoms and solvents and counteranions are omitted.

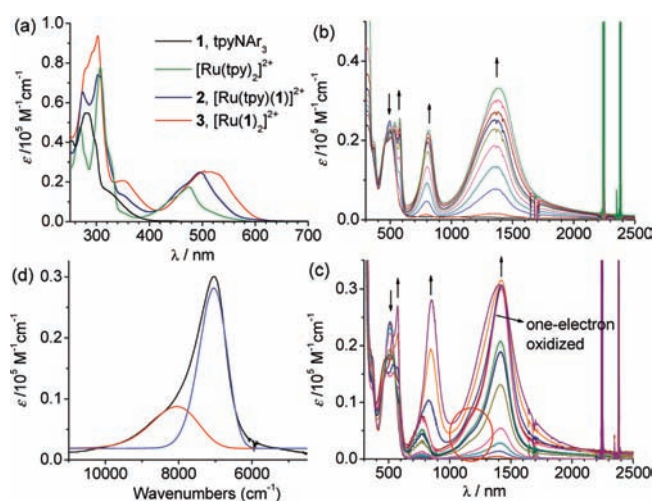


Figure 2. (a): UV/vis absorption spectra of **1–3** in CH_2Cl_2 and $[\text{Ru}(\text{tpy})_2](\text{PF}_6)_2$ in acetonitrile; (b) and (c): UV/vis/NIR electronic absorption spectral changes of **2** (b) and **3** (c) CH_2Cl_2 after gradual addition of SbCl_5 ; (d): Deconvoluted IVCT transition band (red line) of MV complex of **3**.

to the N/N^{*+} process of the di-*p*-anisylamino moiety, and the latter peak is assigned to the $\text{Ru}^{\text{II/III}}$ process, which overlaps with the irreversible $\text{N}^{*+}/\text{N}^{2+}$ oxidation at +1.35 V. The relatively

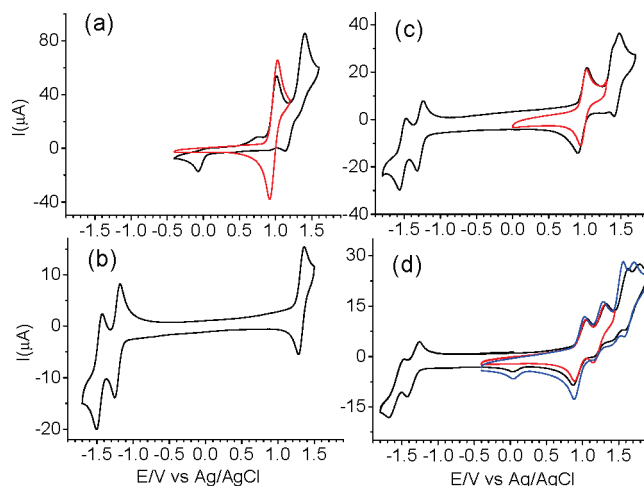


Figure 3. CVs of **1** (a), $[\text{Ru}(\text{tpy})_2](\text{PF}_6)_2$ (b), **2** (c), and **3** (d) in a mixture of acetonitrile/ CH_2Cl_2 (1:1) containing 0.1 M Bu_4NClO_4 as the supporting electrolyte at a scan rate of 100 mV s^{-1} .

larger cathodic current than the anodic current of the peak at +0.98 V in the black line of Figure 2c is probably a result of the contamination caused by the irreversible $\text{N}^{*+}/\text{N}^{2+}$ process. However, this is not an issue when the potential was scanned back before the $\text{N}^{*+}/\text{N}^{2+}$ process (red line). It is noteworthy that the $\text{Ru}^{\text{II/III}}$ process of **2** is 120 mV more positive than that of $[\text{Ru}(\text{tpy})_2](\text{PF}_6)_2$ (Figure 3b). This suggests that the di-*p*-anisylamino unit is positively charged and withdraws the electron density from the metal center.

CV profiles of complex **3** are shown in Figure 3d. The first two redox couples at +0.96 and +1.23 V vs Ag/AgCl could be ascribed to the stepwise oxidation of two di-*p*-anisylamino units into corresponding radical-cation species. The potential separation (ΔE) between two peaks is 270 mV. The comproportionation constant¹⁵ K_c for the equilibrium $[\text{N}-\text{Ru}^{\text{II}}-\text{N}] + [\text{N}^{*+}-\text{Ru}^{\text{II}}-\text{N}^{*+}] \leftrightarrow [\text{N}-\text{Ru}^{\text{II}}-\text{N}^{*+}]$ is 2.55×10^4 , which indicates the high thermodynamic stability of the electrochemically generated MV compound $[\text{N}-\text{Ru}^{\text{II}}-\text{N}^{*+}]$. The irreversible peak at +1.56 V is attributable to the further oxidation of the in situ produced ammonium radical cations, as is found in free ligand **1**. The reversible redox couple at +1.64 V is ascribed to the $\text{Ru}^{\text{II/III}}$ process of **3**. This process occurs at a more positive potential than that of **2** and $[\text{Ru}(\text{tpy})_2](\text{PF}_6)_2$ because of the presence of two appended ammonium cations. The cathodic scans of **2** and **3** both display two redox couples from the reduction of tpy ligands. It is clear that the electrochemical energy gap of **2** or **3**, determined by the potential difference between the first anodic and first cathodic peaks, is narrower than that of $[\text{Ru}(\text{tpy})_2](\text{PF}_6)_2$.

To further probe the electronic delocalization of **2** and **3**, their UV/vis/near-IR (NIR) absorption spectral changes upon the gradual addition of a SbCl_5 solution in CH_2Cl_2 are monitored (Figure 2b,c). Upon the gradual addition of the oxidant, the di-*p*-anisylamino unit in complex **2** was stepwisely oxidized to N^{*+} , as evidenced by the emergence of a new band at 810 nm arising from a typical triarylamine radical-cation species.⁴ At the same time, the MLCT/LLCT transitions display a slight red shift and an intense band at 1360 nm appears. The latter peak is assigned to an electron transfer from the metal component to the triarylamine center ($\text{M} \rightarrow \text{N}^{*+}$). The observation of a clear

isosbestic point at 520 nm suggests a clean conversion of the N/N^{*+} process. A further addition of $SbCl_5$ causes no further change of the spectrum.

The absorption spectral changes of complex **3** in response to the addition of $SbCl_5$ are shown in Figures 2c and S5 and S6 in the Supporting Information. Upon the gradual addition of the oxidant, one of the di-*p*-anisylamino sites was first oxidized to the N^{*+} species. The absorption spectrum shows changes similar to those in complex **2** except that a clear shoulder band around 1160 nm grows gradually (highlighted with a red circle). Upon a further addition of the oxidant, the second triarylamino unit was oxidized as well. The previously observed shoulder disappears gradually, and the N^{*+} band around 800 nm shifts bathochromically slightly. On the basis of these facts, the shoulder band at 1160 nm is assigned to the IVCT transition of the chemically generated MV complex of **3**. Part of the NIR transitions of the one-electron-oxidized intermediate of complex **3** is shown in Figure 2d. Because the IVCT band is overlapped with the intense $M \rightarrow N^{*+}$ transition (around 1400 nm), we assume that the IVCT band is symmetrical and Gaussian-shaped. Thus, the black line from the experimental data is deconvoluted into the IVCT band (red line) and the $M \rightarrow N^{*+}$ transition (blue line), as shown in Figure 2d. The IVCT band centers at 1240 nm ($\nu_{\max} = 8050 \text{ cm}^{-1}$) with ϵ_{\max} of $8700 \text{ M}^{-1} \text{ cm}^{-1}$ and a full width at half-height ($\Delta\nu_{1/2}$) of 1800 cm^{-1} . The electronic coupling parameter H_{ab} is estimated to be 600 cm^{-1} , according to the Hush formula: $H_{ab} = 0.0206 \cdot (\epsilon_{\max} \nu_{\max} \Delta\nu_{1/2})^{1/2} / r_{ab}$,¹⁶ where r_{ab} is the diabatic electron-transfer distance and is taken to be the intramolecular N–N crystallographic distance (d_{N-N} , 12.26 Å). It should be noted that the true r_{ab} may be much shorter than d_{N-N} because of delocalization of the charge from the amine site into the bridging group.¹⁷ Thus, the calculated H_{ab} value is likely to be a lower limit. This value is on the same order with those for mixed-valent di-*p*-anisylamines bridged by $C_6H_4C \equiv CC_6H_4C \equiv CC_6H_4$,^{4c} $C_6H_4C \equiv CPtC \equiv CC_6H_4$,⁹ or $C_6H_4C \equiv CC \equiv CC_6H_4$.^{4c} However, it is lower than those for mixed-valent di-*p*-anisylamines bridged by $C_6H_4C \equiv CC_6H_4$ ^{4c} or $C_6H_4CH = CHC_6H_4$ ^{4b} with similar N–N distances. Finally, it was found that one-electron-oxidized species of both **2** and **3** show clear electron paramagnetic resonance (EPR) signals at 77 K with *g* factors of 2.044 and 2.002 (Figures S7 and S8 in the Supporting Information), respectively. This supports that the spin is largely nitrogen-centered. However, the observation of a discernible axial splitting ($g_1 = 2.043$) of complex **3** after one-electron oxidation points to an appreciable metal character of the free radical.

To conclude, the electronic communication between two di-*p*-anisylamines bridged by a $[Ru(\text{tpy})_2]$ motif was estimated by analyzing the IVCT band of the corresponding MV monoradical-cation species. As illustrated in this contribution, the concept of assembling organic redox centers with transition-metal complexes as the bridge, instead of the conventional M–BL–M arrangement (M refers to an organometallic or inorganic redox center and BL is an organic bridge), is important for the future design and synthesis of new types of MV systems. The quantification of the electronic coupling between two amine redox sites bridged by linear transition-metal complexes provides useful information in terms of their applications as conducting molecular wires.

ASSOCIATED CONTENT

S Supporting Information. Syntheses and characterization, NMR spectra of new compounds, CV profiles of **1–3**, CIF file of **3**, plots of spectral changes of **3** upon oxidation, and

EPR plots of **2** and **3** after one-electron oxidation. This material is available free of charge via the Internet at <http://pubs.acs.org>.

AUTHOR INFORMATION

Corresponding Author

*E-mail: zhongyuwu@iccas.ac.cn.

ACKNOWLEDGMENT

We thank the National Natural Science Foundation of China (Grant 21002104), the National Basic Research 973 program of China (Grant 2011CB932301), and the Institute of Chemistry, Chinese Academy of Sciences (“100 Talent” Program), for funding support.

REFERENCES

- (1) (a) D’Alessandro, D. M.; Keene, F. R. *Chem. Rev.* **2006**, *106*, 2270. (b) Kaim, W.; Lahiri, G. K. *Angew. Chem., Int. Ed.* **2007**, *46*, 1778.
- (2) Aguirre-Etcheverry, P.; O’Hare, D. *Chem. Rev.* **2010**, *110*, 4839.
- (3) Nelsen, S. E. *Chem.—Eur. J.* **2000**, *6*, 581.
- (4) (a) Zhou, G.; Baumgarten, M.; Müllen, K. *J. Am. Chem. Soc.* **2007**, *129*, 12211. (b) Barlow, S.; Risko, C.; Chung, S.-J.; Tucker, N. M.; Coropceanu, V.; Jones, S. C.; Levi, Z.; Brédas, J.-L.; Marder, S. R. *J. Am. Chem. Soc.* **2005**, *127*, 16900. (c) Lambert, C.; Nöll, G. *J. Am. Chem. Soc.* **1999**, *121*, 8434. (d) Lambert, C.; Nöll, G.; Schelter, J. *Nat. Mater.* **2002**, *1*, 69. (e) Barlow, S.; Risko, C.; Coropceanu, V.; Tucker, N. M.; Jones, S. C.; Levi, Z.; Khrustalev, V. N.; Antipin, M. Y.; Kinniburgh, T. L.; Timofeeva, T.; Marder, S. R.; Brédas, J.-L. *Chem. Commun.* **2005**, 764. (f) Lambert, C.; Risko, C.; Coropceanu, V.; Schelter, J.; Amthor, S.; Gruhn, N. E.; Durivage, J. C.; Brédas, J.-L. *J. Am. Chem. Soc.* **2005**, *127*, 8508.
- (5) Ning, Z.; Tian, H. *Chem. Commun.* **2009**, 5483.
- (6) (a) Schubert, S. S.; Eschbaumer, C. *Angew. Chem., Int. Ed.* **2002**, *41*, 2892. (b) Eryazici, I.; Moorefield, C. N.; Newkome, G. R. *Chem. Rev.* **2008**, *108*, 1834. (c) Constable, E. C. *Chem. Soc. Rev.* **2007**, *36*, 246.
- (7) Flores-Torres, S.; Hutchison, G. R.; Stoltzberg, L. J.; Abruña, H. D. *J. Am. Chem. Soc.* **2006**, *128*, 1513.
- (8) Sakamoto, R.; Sasaki, T.; Honda, N.; Yamamura, T. *Chem. Commun.* **2009**, 5156.
- (9) Jones, S. C.; Coropceanu, V.; Barlow, S.; Kinniburgh, T.; Timofeeva, T.; Brédas, J.-L.; Marder, S. R. *J. Am. Chem. Soc.* **2004**, *126*, 11782.
- (10) Robson, K. C. K.; Koivisto, B. D.; Gordon, T. J.; Baumgartner, T.; Berlinguette, C. P. *Inorg. Chem.* **2010**, *49*, 5335.
- (11) Yang, J.-S.; Lin, Y.-H.; Yang, C.-S. *Org. Lett.* **2002**, *4*, 777.
- (12) Crystallographic data for $(3)_2(\text{CHCl}_3)_{13}(\text{NO}_3)_4 \cdot \text{C}_{129}\text{H}_{109}\text{Cl}_{39}\text{N}_{20}\text{O}_{20}\text{Ru}_2$, $M = 3844.05$, triclinic, $a = 10.858(2) \text{ \AA}$, $b = 18.726(4) \text{ \AA}$, $c = 20.548(4) \text{ \AA}$, $\alpha = 97.57(3)^\circ$, $\beta = 102.43(3)^\circ$, $\gamma = 90.03(3)^\circ$, $U = 4042.3(14) \text{ \AA}^3$, $T = 173 \text{ K}$, space group $P\bar{1}$, $Z = 1$, 11 514 reflections measured, radiation type Mo $K\alpha$, radiation wavelength 0.71073 \AA , final R indices $R1 = 0.1242$ and $wR2 = 0.3267$, and R indices (all data) $R1 = 0.1329$ and $wR2 = 0.3380$.
- (13) Sreenath, K.; Thomas, T. G.; Gopidas, K. R. *Org. Lett.* **2011**, *13*, 1134.
- (14) Matis, M.; Rapta, P.; Lukeš, V.; Hartmann, H.; Dunsch, L. *J. Phys. Chem. B* **2010**, *114*, 4451.
- (15) $K_c = 10^{AE(mV)/59}$ for a room temperature case. See ref 1.
- (16) (a) Hush, N. S. *Prog. Inorg. Chem.* **1967**, *8*, 391. (b) Hush, N. S. *Coord. Chem. Rev.* **1985**, *64*, 135.
- (17) Heckmann, A.; Amthor, S.; Lambert, C. *Chem. Commun.* **2006**, 2959.